UNIVERSIDAD NACIONAL DE COLOMBIA
SEDE MEDELLÍN
FACULTAD DE MINAS

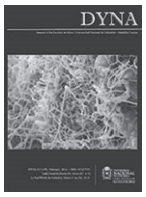

DYNA
http://dyna.medellin.unal.edu.co/

Non-destructive *in situ* analysis of garnet by combining scanning electron microscopy and X-ray diffraction techniques

John Deiver Bonilla-Jaimes [a], Jose Antonio Henao-Martínez [a], Carolina Mendoza-Luna [b], Oscar Mauricio Castellanos-Alarcón [c] & Carlos Alberto Ríos-Reyes [d]

[a] *Escuela de Química, Universidad Industrial de Santander, Bucaramanga, Colombia, johnrayosx@gmail.com*
[a] *Escuela de Química, Universidad Industrial de Santander, Bucaramanga, Colombia, jahenao@uis.edu.co*
[b] *Escuela de Física, Universidad Industrial de Santander, Bucaramanga, Colombia, caroluna8007@gmail.com*
[c] *Programa de Geología, Universidad de Pamplona, Pamplona, Colombia, oscarmca@yahoo.es*
[d] *Escuela de Geología, Universidad Industrial de Santander, Bucaramanga, Colombia, carios@uis.edu.co*

Received: October 19th, 2014.Received in revised form: August 11th, 2015. Accepted: January 21th, 2016.

Abstract
By using the X-ray powder diffraction (XRPD) micro X-rays diffraction (μXRD) and scanning electron microscopy, the structural characterization of minerals is far more reliable and accurate. The identification and elemental and compositional quantification of minerals by these non-destructive techniques improve the quality of the results and allow a full analysis of the material. The data obtained by these techniques revealed the presence of garnet-type spessartine, in addition to trace elements and compounds that form the overall material. The structural refinement of spessartine was performed using the Rietveld method from data obtained by conventional diffraction and by using the MDI RIQAS analysis software. With the data acquired by μXRD using an area detector, a shorter exposure time (compared to that required by the 0L and 1D detectors) was achieved, and there was no need for particle size reduction of the mineral. It was also possible to identify the spessartine and other compounds in smaller concentrations (in situ measurements). By combining scanning electron microscopy and X-ray diffraction techniques, both worked from a characterization point of view. The examination by micro X-ray diffraction did not require physical separation of the sample. Using this information and the above advanced analytical techniques, the identification of garnet can be undertaken much more reliably.

Keywords: scanning electron microscopy; micro X-ray diffraction; analytical techniques; mineral; garnet.

Análisis no destructivos *in situ* de granate, combinando las técnicas de microscopía electrónica de barrido y difracción de rayos-X

Resumen
Mediante el uso de la difracción de rayos-X de polvo (DRXP), microdifracción de rayos-X (μDXR) y microscopía electrónica de barrido, la caracterización estructural de minerales resulta ser mucho más fiable y precisa. La identificación y cuantificación elemental y composicional de los minerales mediante estas técnicas no destructivas, mejoran la calidad de los resultados y permiten realizar un análisis completo del material. Los datos obtenidos mediante estas técnicas revelaron la presencia de granate tipo espesartina, además de los elementos y compuestos trazas que conforman el material en general. El refinamiento estructural de la espesartina fue realizado mediante el método Rietveld a partir de los datos obtenidos por difracción convencional y con ayuda del software de análisis MDI RIQAS. Con los datos adquiridos por μDXR usando un detector de área, un menor tiempo de exposición (comparado con el requerido en detectores 0D y 1D) y sin la necesidad de la disminución del tamaño de partícula del mineral, fue posible la identificación de la espesartina y otros compuestos en menor concentración (mediciones "in situ"). Mediante la combinación de las técnicas de microscopía electrónica de barrido y microdifracción de rayos X, tanto de trabajo desde un punto de vista de la caracterización. El examen por difracción de micro-rayos X no requiere la separación física de la muestra. Usando esta información y las técnicas analíticas avanzadas anteriores, la identificación de granate puede ser mucho más fiable.

Palabras claves: microscopía electrónica de barrido; micro difracción de rayos-X; técnicas analíticas; mineral; granate.

1. Introduction

The destructive character of many analytical techniques has restricted studies in mineral characterization, since the conservation of mineral properties has been prioritized above any information that may be obtained. However, the continuous improvements in scientific instruments has made it possible to study minerals in a non-destructive way, without any degradation or alteration in their appearance. The scanning electron microscopy (SEM) and X-ray diffraction (XRD and μXRD) techniques enable the mineral characterization in a non-destructive way. The μXRD is a structural analysis technique that allows very small sample areas to be examined to obtain information about the structure of crystalline materials. Recent developments in specialized laboratories have extended the application of μXRD to the examination of geomaterials, which have a broad spectrum of applications [1] in the fields of mineralogy [2], petrology [3], material sciences, environmental sciences [4], and Earth and planetary sciences [5-8]. The SEM is a powerful tool for the microstructural analysis of geomaterials. The μXRD is a versatile technique that uses a two-dimensional (2D) general area detector diffraction system (GADDS), which acquires textural and crystallinity information and easily discriminates between multiple phases, providing mineral identification using crystal structural parameters [5]. Moreover, in situ μXRD of minerals preserves spatial relationships, enabling the study of orientational phenomena, such as strain-related mosaicity (giving "streaked" diffraction lines). The objective of this study is to carry out the analysis of garnet by combining SEM and μXRD techniques.

2. Analytical techniques

2.1. Materials

The sample that was analyzed is from a garnet amphibolite from the Arquía Complex, cropping out on the southern Pijao (Quindío). Several studies [9-12] report the occurrence of this type of rock in the Arquía Complex, which represents a tectonic mixture of blocks of different origins (e.g., oceanic crust, subduction zone, marine sedimentary rocks, etc.) that were created by the shearing zone between the Caribbean-Colombian Cretaceous Igneous Province and the Colombian western margin during the Cretaceous period [13]. According to Kerr et al. [14], these processes result in the formation of ophiolitic complexes, metamorphic belts and the amalgamation and strong interaction of several tectonic terranes.

2.2. Analysis

2.2.1. Petrographic analysis

The garnet amphibolite samples were first analyzed by transmitted light microscopy, by using a Nikon trinocular microscope (model Labophot2-POL) in order to capture photomicrographs with the 5x objective of the optical properties of garnet, as well as its textural relationships with other mineral phases. The Kretz [14] system of mineral abbreviations is used.

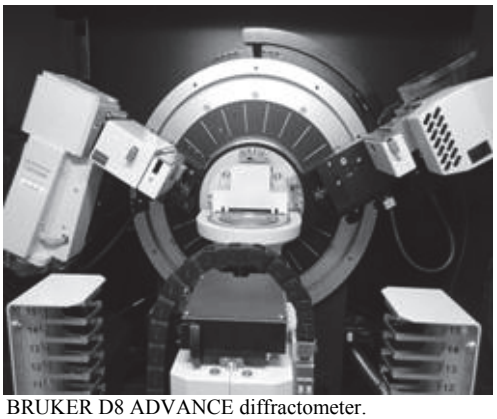

Figure 1. BRUKER D8 ADVANCE diffractometer.
Source: The authors.

2.2.2. Scanning electron microscopy (SEM)

Backscatter electron (BSE) imaging and EDS analysis of garnet were carried out using a FEI QUANTA FEG 650 environmental scanning electron microscope (ESEM), under the following analytical conditions: magnification = 100-20000x, WD = 9.0-11.0 mm, HV = 20 kV, signal = BSE in Z CONT mode, detector = BSED, EDS Detector EDAX APOLO X with resolution of 126.1 eV (in. Mn Kα).

2.2.3. X-ray powder diffraction (XRPD)

The sample was milled in an agate mortar and then mounted on a sample holder of polymethylmethacrylate (PMMA) using the filling front technique . The XRPD pattern of garnet was recorded by X-ray diffraction using a BRUKER D8 ADVANCE diffractometer (Fig. 1) operating in Da Vinci geometry and equipped with an X-ray tube (Cu-Kα1 radiation: λ = 1.5406 Å, 40 kV and 30 mA), a 1-dimensional LynxEye detector (with aperture angle of 2.93º), a divergent slit of 0.6 mm, two soller axials (primary and secondary) of 2.5º and a nickel filter. Data collection was carried out in the 2θ range of 12-80°, with a step size of 0.01526° (2θ) and counting time of 1 s/step. Phase identification was performed using the crystallographic database Powder Diffraction File (PDF-2) from the International Centre for Diffraction Data (ICDD) and the Crystallographica Search-Match program. The unit-cell constants, atomic positions, factors of peak broadening and phase concentrations were refined and calculated by using the MDI RIQAS program based on Rietveld method.

2.2.4. Micro X-Ray Diffraction (μXRD)

For a powder sample measurement, an agate mortar was first milled and then mounted on a polymethylmethacrylate (PMMA)sample holder using the filling front technique. Finally, the measurement was adjusted in the Eulerian cradle.

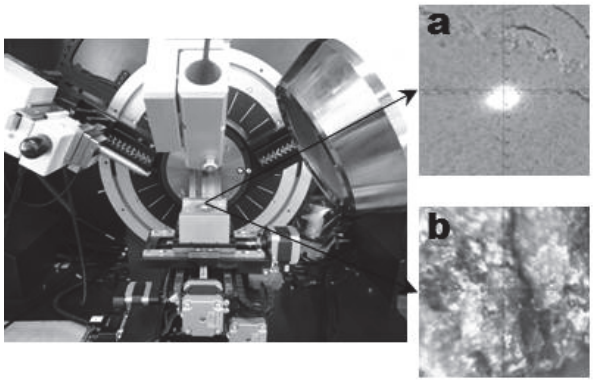

Figure 2. BRUKER D8 DISCOVER XRD^2 diffractometer. (a) μXRD on the milled simple. (b) μXRD on the unmilled sample.
Source: The authors.

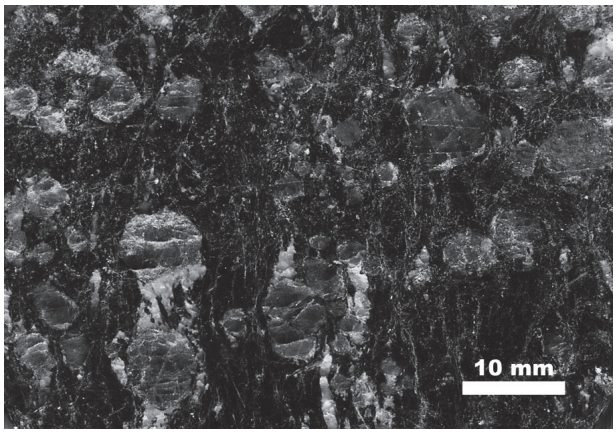

Figure 3. Photograph of the garnet amphibolite's hand specimen.
Source: The authors.

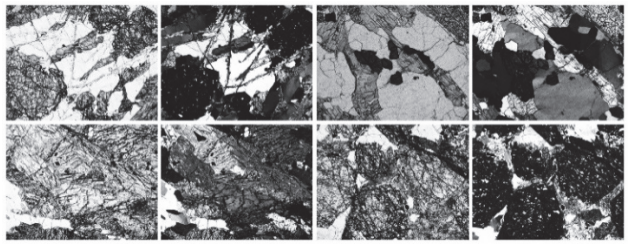

Figure 4. Photomicrographs of the garnet amphibolite observed under a transmitted light microscope. Grt, garnet; Hbl, hornblende; Qtz, quartz; Ilm, ilmenite; Cpy, chalcopyrite; Zrn, zircon; Chl, chlorite.
Source: The authors.

To measure an unmilled sample, the XYZ coordinate system of the quarter-circle Eulerian cradle was adjusted directly. μXRD data on powder and unmilled samples were collected with the BRUKER D8 DISCOVER diffractometer, equipped with the 2D GADDS (Fig. 2), operated in Da Vinci geometry with CuKα1 radiation (λ = 1.5406 Å) at 40 kV and 30 mA; equipped with a Optics Göebel Mirror, a circular divergent slit of 1 mm, a collimator of 1 mm, and a 2-dimensional detector VÅNTEC-500 (with an angular aperture of 42º in the 2θ range and a work distance of 150 mm). Data collection was carried out in the 2θ range of 25-45° in two intervals, with an increase per interval of 20° (2θ), a step scan, and a pixel size of 2048 x 2048. The two dimensional (2D) image GADDS were obtained in the spherical coordinate system of the Debye-Scherrer rings by using the DIFFRACT PILOT program. The diffraction patterns were obtained from the integration of several sections of the Debye-Scherrer rings by using a 0.01º (2θ) step. Phase identification was performed using the crystallographic database Powder Diffraction File (PDF-2) from the International Centre for Diffraction Data (ICDD) and the Crystallographica Search-Match software.

3. Results

3.1. Petrographic analysis

Fig. 3 shows a photograph of the garnet amphibolite of interest in the present study's hand specimen, with the garnet being typically dark reddish brown in color with a vitreous luster and xenoblastic character. It develops large porphyroblasts in a dark green nematoblastic matrix and is mainly composed of hornblende.

Fig. 4 illustrates the corresponding photomicrographs with large xenoblastic garnet porphyroblasts in a matrix mainly composed of hornblende.

3.2. Scanning electron microscopy (SEM)

The backscatter electron (BSE) images Figs. 5-6 show the textural relationships observed between spessartine-type garnet and associated mineral phases with semiquantitative energy dispersive spectrum (EDS) analysis at different points. This allowed particular elements and their relative proportions in the mineral phases that constitute the garnet-amphibolite sample of interest in this study to be identified. EDS analysis reveals that the main mineral phases in the analyzed rocks correspond to spessartine-type garnet and hornblende. The main accessory mineral phases are quartz, zoisite (epidote-group mineral), rutile, ilmenite, pyrite, chalcopyrite and zircon. Chlorite is recognized as a replacement product of hornblende.

Fig. 5a illustrates examples of the matrix mineral phases, with hornblende (1) as the main associated mineral phase, which is commonly replaced by chlorite (2). Rutile (3) developing reaction rims of titanite (4) occurs as the main accessory mineral phase. Very fine-grained zircon (5) crystals are scarcely distributed in the study samples. EDS analysis reveals the following mass ratios: Si:Al:O:Fe:Ca:Mg:Na:K:Ti for hornblende (23.64:6.98:26.91:11.44:6.90:6.73:1.59:0.29:0.29), Si:Al:O:Fe:Mgfor chlorite (14.11:10.91:31.58:19.18:9.91), Ti:O for rutile (64.40:26.49), Si:Al:O:Ca:Ti:Fe for titanite (15.91:0.51:22.39:22.10:28.68:0.33), and Si:O:Zr for zircon (15.62:18.38:45.25). Fig. 5b displays the occurrence of numerous randomly distributed mineral inclusions, such as quartz (6), zoisite (7), hornblende (8), chalcopyrite (9) and ilmenite (10), in spessartine-type garnet. EDS analysis reveals the following mass ratios: Si:O for quartz (47.34:35.62), Si:Al:O:Ca:Fe for zoisite (19.86:15.3726.96:17.11:6.38), Si:Al:O:Mg:Fe for hornblende (13.36:11.11:33.09:11.14:16.00), Fe:Cu:S for chalcopyrite (24.91:28.72:27.65), and Ti:Fe:O for ilmenite (30.93:37.65:20.75).

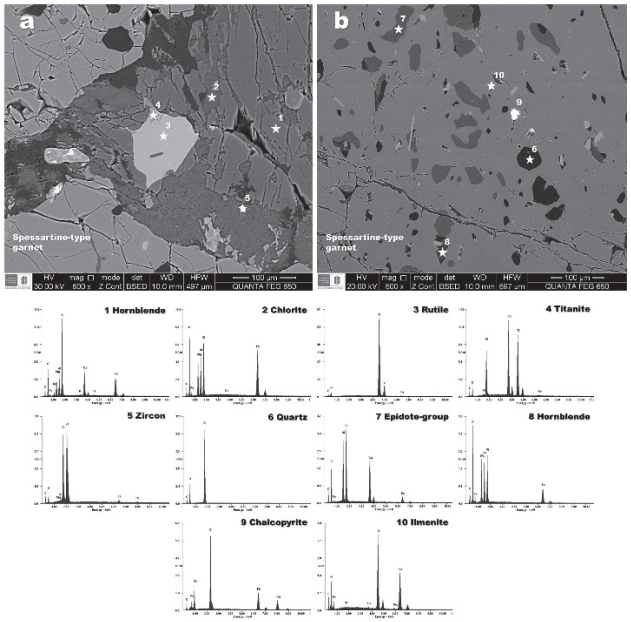

Figure 5. SEM photomicrographs and EDS spectra at the marked stars on the images of the mineral phases associated with spessartine-type garnet. The appearance of C element was attributed to the carbon coating on the sample before SEM analysis.
Source: The authors.

Figs. 6a and 6b illustrate the occurrence of pyrite (1) in the matrix, which contains chalcopyrite (2) inclusions and is partially replaced by leucoxene (3). Figs. 6c and 6d illustrate the occurrence of ilmenite (4) in the matrix, which contains zoisite (5) inclusions and is partially replaced by rutile (6). EDS analysis reveals the following mass ratios: Fe:S for pyrite (38.38:41.25), Fe:Cu:S for chalcopyrite (24.91:28.72:27.65), Fe:O for leucoxene (66.22:19.87),

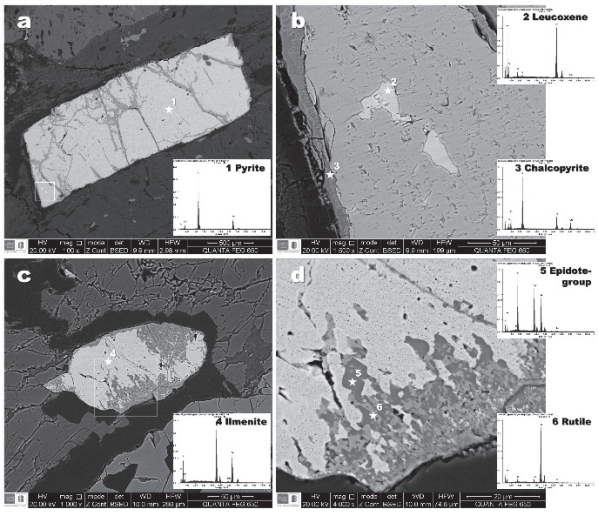

Figure 6. SEM photomicrographs and EDS spectra at the marked stars on the image of the Fe-Ti oxide mineral phases associated with spessartine-type garnet. The appearance of C element attributed to the carbon coating on the sample before SEM analysis.
Source: The authors.

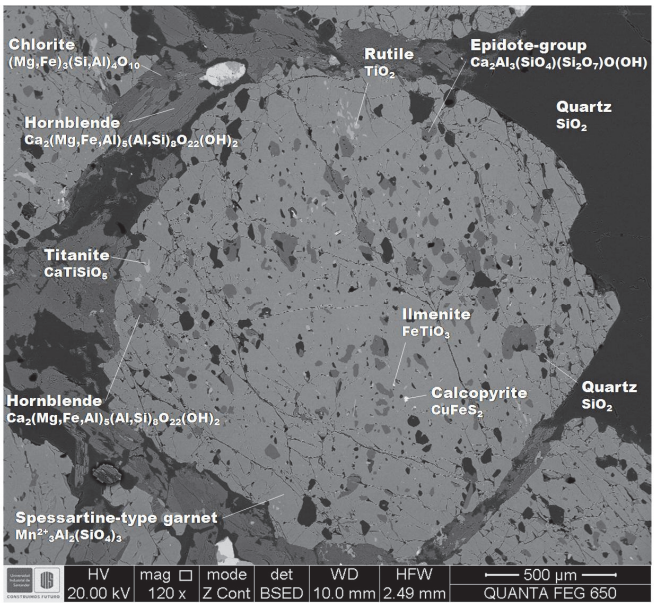

Figure 7. BSE image of spessartine-type garnet. Variation in intensity of grey scale color shows a rough variation in mineral chemistry.
Source: The authors.

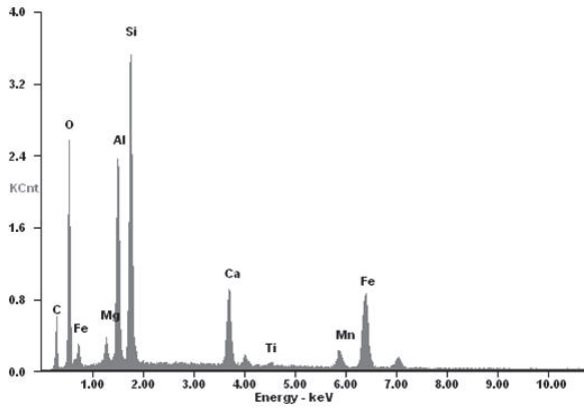

Figure 8. EDS spectrum of spessartine-type garnet. The appearance of C element is attributed to the carbon coating on the sample before SEM analysis.
Source: The authors.

Ti:Fe:O for ilmenite (30.93:37.65:20.75),Si:Al:O:Ca:Ti:Fe for zoisite (16.92:0.44:23.90:21.36:25.47:0.93), and Ti:O for rutile (64.40:26.49).

The backscatter electron (BSE) image Fig. 7 shows the textural relationships observed between spessartine-type garnet and associated mineral phases. Note the high-density Fe-Ti oxide (on the upper and lower parts), the randomly oriented inclusion-rich spessartine-type garnet and associated mineral phases, and the reaction textures from the BSE image contrast.

EDS analysis reveals that the mass ratios (Si:Al:O:Fe:Ca:Mn:Mg) of the spessartine-type garnet are 18.96:11.63:25.49:18.50:6.32:3.67:1.56. The EDS spectrum of spessartine-type garnet (Fig. 8) reveals that it mainly consists of Si, Al, O, Fe and Ca, with a minor amount of Mn and Mg.

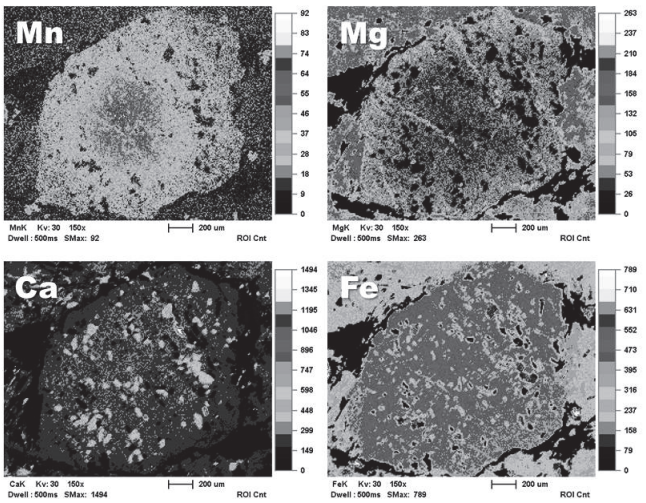

Figure 9. (a) Mn, (b) Mg, (c) Ca and (d) Fe compositional maps of spessartine-type garnet and associated mineral phases. Light colors show areas of high concentration while dark colors represent areas of low concentration (black is very low concentration).
Source: The authors.

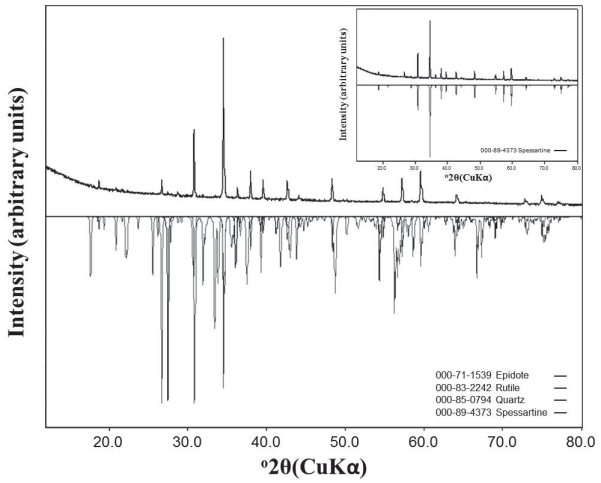

Figure 10. XRPD pattern of spessartine-type garnet. In the lower part shows the diffraction patterns of the mineral phases identified in the crystallographic database Powder Diffraction File (PDF-2) from the International Centre for Diffraction Data (ICDD).
Source: The authors.

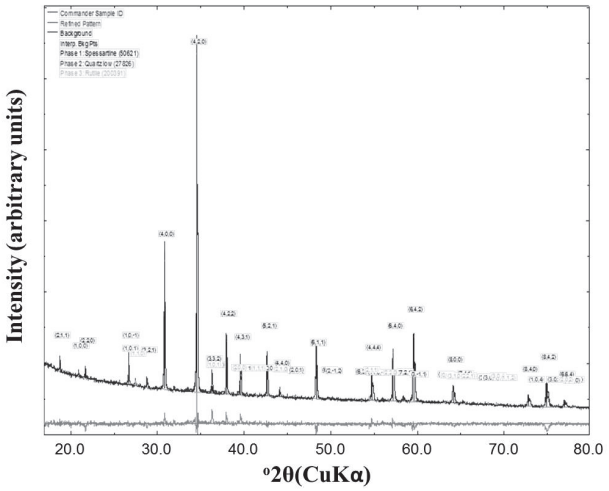

Figure 11. Observed (cross-hatches) and calculated (continuous lines) profiles and the corresponding difference diagram of spessartine-type garnet (λ = 1.5406 Å).
Source: The authors.

X-rays generated by scanning the electron beam across the sample can be used to produce EDS mapping, which provides an image of a meaningful picture of the elemental distribution of a mineral phase, in addition to the BSE. In Fig. 9, the different phases shown on the BSE image (Fig. 9a) can be identified by elemental mapping (Figs. 9b-9d); however, this will only give a qualitative image of the distribution of elements. The elemental mapping shows an oscillatory pattern with respect to Mn (Fig. 9b, X_{sps}), which has a decrease of X_{sps}. However, this cannot be attributed to the abundant epidote-group inclusions, because there is no relationship between zoning and the distribution pattern of inclusions. No chemical zoning can be identified from the core to the rim with regards to Mg (Fig. 9c, X_{grs}) and Ca (Fig. 9d, X_{grs}).

Elemental maps provide valuable information even without μXRD. It is very important to highlight that a high Mn content is mirrored by a low Mg content. Note the high content of Ca, representing zoisite (a Ca-rich mineral phase) inclusions in the spessartine-type garnet. Fe content is very uniform in spessartine-type garnet; however, the low Fe content of the mineral inclusions should be noted.

3.3. X-ray powder diffraction (XRPD)

Fig. 10 shows the XRPD pattern of the spessartine-type garnet, in which the high intensity reflections correspond to spessartine-type garnet (PDF No. 000-89-4373), and the low intensity reflections reveal the presence of quartz (PDF No. 000-89-0794), rutile (PDF No. 000-83-2242), and epidote (PDF No. 000-71-1539).

The Rietveld refinement of the XRPD pattern allows the percentage of the rock-forming minerals to be determined. Fig. 11 illustrates the observed, calculated and difference profiles for the XRPD garnet data after refinement. The crystalline phase of interest in this study corresponds to a spessartine-type garnet structure, although a few extra lines reveal the occurrence of other mineral phases that are described above. The difference between the observed and calculated profiles shows a good fit for the refined parameters (cell-unit constants, atomic positions, factors of peak broadening and phase concentrations).

The Rietveld refinement details (including the parameters of profile broadening U, V, W, m), obtained for the spessartine-type garnet, are presented in Table 1. The refinement of the XRPD data reveals a small preferential orientation in the reflection (400) for the spessartine-type garnet framework, which crystallized in the cubic space

Table 1.
The Rietveld refinement details obtained for the spessartine-type garnet.

Molecular formula	$(Mn_{2.21}Fe0_{.79})Al_2(SiO_4)_3$
Molecular weight (g/mol)	495.03
a = b = c (Å)	11.6086
α = β = γ (º)	90
V (Å^3)	1564.37
Z	8
Space group	Ia3̄d
ρ (g/cm^3)	4.208
U	0.146049
V	-0.08092
W	0.016211
m	1.35655
R_{WP} (%)	19.47
R (%)	12.02
R_{exp} (%)	3.4
χ^2	3.2

Source: The authors.

Table 2.
Atomic positions obtained for the spessartine-type garnet.

Atom	Ion	X	Y	Z
Mn1	Mn^{+2}	0	1/4	1/8
Fe1	Fe^{+2}	0	1/4	1/8
Al1	Al^{+3}	0	0	0
Si1	Si^{+4}	0	1/4	3/8
O1	O^{-2}	0.038071	0.043327	0.657748

Source: The authors.

group Ia3̄d (nº 230), and has unit cell parameters a = b = c = 11.6086 Å; α = β = γ = 90º, V = 1564.37 Å^3, Z = 8 and ρ =4.208 g/cm^3. ICSD = 50621 was the number used to refine the spessartine-type garnet. These results fully agree with those obtained by Sawada [15].

The concentrations of the refined phases and their corresponding (standard deviation) obtained were: spessartine-type garnet $(Mn_{2.21}Fe_{0.79})Al_2(SiO_4)_3$ = 94.0% (0.3), quartz (SiO_2) = 4.9% (0.1), rutile (TiO_2) = 1.1% (0.1). The concentration and corresponding standard deviation of the epidote cannot be quantified due to its low concentration.

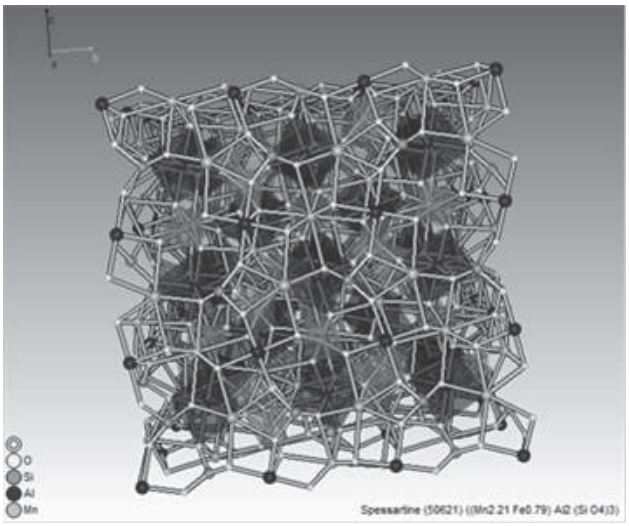

Figure 12. Structure of spessartine-type garnet.
Source: The authors.

The final agreement values for the refinement are R_{wp} = 19.47%, R = 12.02%, R_{exp} = 3.40%, and χ^2 = 3.2.

In the refinement model used in this study, only the atomic coordinates for oxygen were refined with a standard deviation in the three crystallographic axes that was lower than 10% with respect to the values reported in the database. The other elements show fixed positions and, therefore, they were not refined. The atomic coordinates for the spessartine-type garnet are depicted in Table 2.

Fig.12 shows the spessartine-type garnet structure obtained with the software MDI RIQAS5.

3.4. Micro X-Ray Diffraction (μXRD)

The two dimensional image (2θ,γ) from the GADDS detector shows how the spessartine-type garnet appears as homogeneous Debye rings (Fig. 13) of constant intensity, displaying 21 diffraction cones of 21 different planes in its crystalline structure. The diffraction spots and the Debye rings match this structure. The continuous and irregular rings reveal that the sample is polycrystalline, however, its particle size is very coarse.

The crystalline accessory minerals appear as a lower pixel diffraction cone of the quartz crystalline plane (011), and small crystalline spots correspond to rutile and epidote, which are shown in the 2D GADDS image of Fig. 14. The internal rings are characterized by the presence of rutile and epidote. This provides useful information on the scarce number of crystallites in these phases and their low concentration. Microcrystalline quartz appears to produce very thin lines, mostly appearing as a series of tiny connected dots, with some larger point reflections.

On each one of the Debye rings, the structure planes diffracted by the spessartine-type garnet are indicated and the reference area and arrow represent the place where the 1D integration diffraction pattern (Intensity vs. 2θ) was obtained (Fig. 15). The identification of the spessartine-type garnet (PDF No. 000-89-4373) was performed by comparing the observed diffraction pattern with the PDF-2 data base patterns.

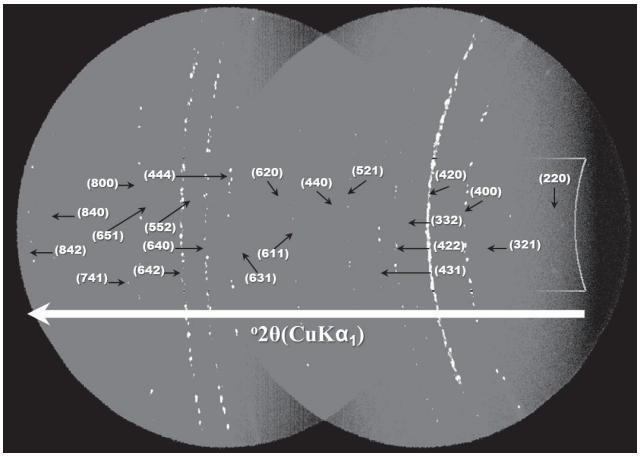

Figure 13. 2D GADDS image of the spessartine-type garnet in the milled sample. The reference area and arrow represent the integration of the 2D GADDS image.
Source: The authors.

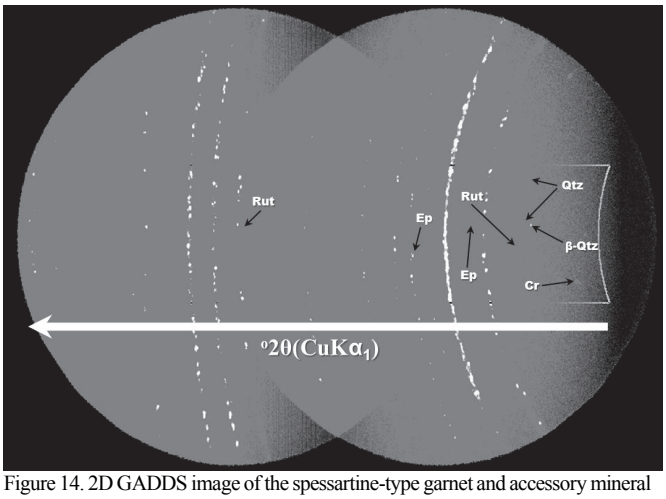

Figure 14. 2D GADDS image of the spessartine-type garnet and accessory mineral phases in the milled sample. The reference area and arrow represent the integration of the 2D GADDS image. Qtz, quartz; Cr, crystoballite; Rut, rutile; Ep, epidote.
Source: The authors.

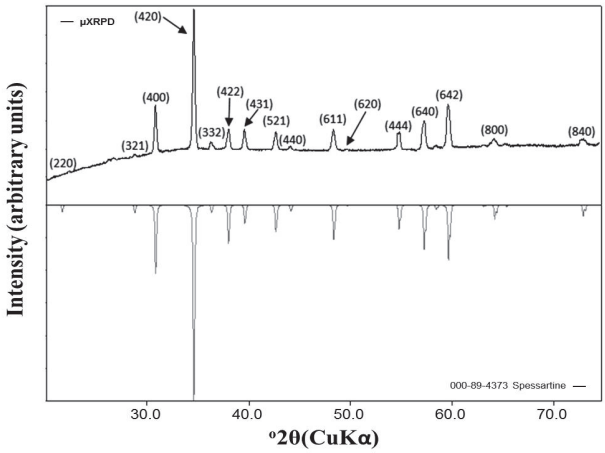

Figure 15. μXRD profile of spessartine-type garnet (λ = 1.5406 Å) in the milled sample, including reflection peaks of mineral inclusions (Qtz, quartz; Cr, crystoballite; Ep, epidote). In the lower part, the XRD diffraction pattern of the spessartine-type garnet, reported by the International Centre for Diffraction Data (ICDD), is shown.
Source: The authors.

μXRD on the unmilled simple reveals the occurrence of spots and discontinue diffraction rings (Fig. 16), which reveals that there is a mixture of crystallites with several sizes and some strong orientations (reflection (840)). The hkl planes observed correspond to the characteristic reflections of the spessartine-type garnet.

In order to observe numerous reflections, it is necessary to rotate the sample at different angles; however, in our case with the eight (8) reflections that were observed, the identification of mineral phases (Fig. 17) was easy.

4. Conclusions

Both scanning electron microscopy and X-ray diffraction techniques are very useful for mineral characterization. Novel analytical methods such as the μXRD technique provide

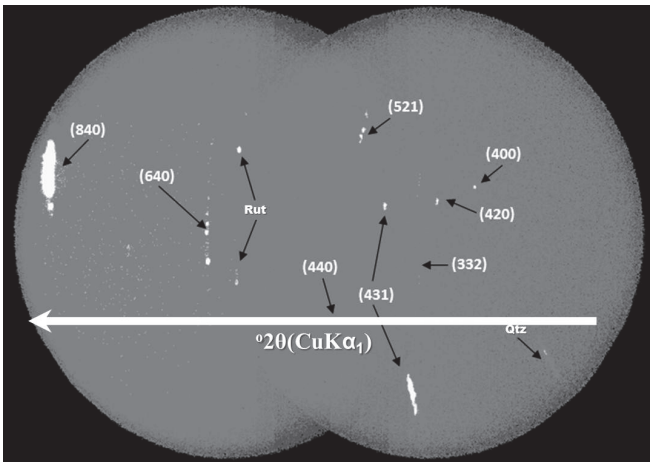

Figure 16. Integration of 2D GADDS image (1D Intensity vs. 2θ plot) and 2D GADDS image of the spessartine-type garnet and accessory mineral phases in the unmilled sample. The diffraction spots and the Debye rings match this structure. Qtz, quartz; Rut, rutile.
Source: The authors.

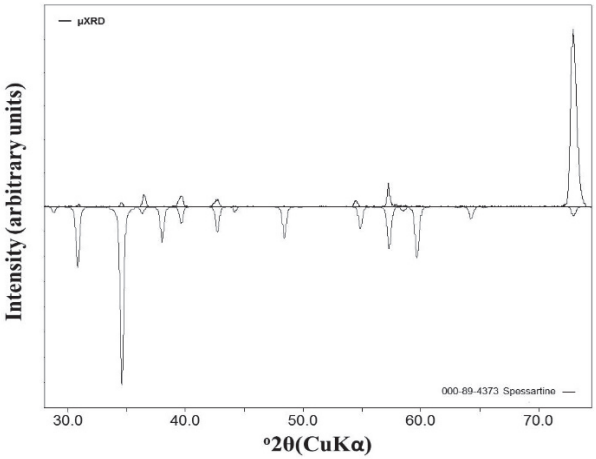

Figure 17. The corresponding μXRD profile of spessartine-type garnet (λ = 1.5406 Å) in the unmilled sample. In the lower part, the diffraction pattern of the spessartine-type garnet is shown, which is reported in the crystallographic database Powder Diffraction File (PDF-2) from the International Centre for Diffraction Data (ICDD). There is a maximum diameter of irradiated sample of 1 mm.
Source: The authors.

the possibility of non-destructive in situ characterization of geological materials with micro spatial resolution. The results in this paper demonstrated the importance of combining such advanced techniques to accurately characterize the distribution of key elements and rock-forming minerals. In this case, analyses were made using (1) petrographic analysis, (2) SEM/EDS analysis, (3) 2-D μXRD (GADDS) representation (4) 1-D μXRD representation. To the best of our knowledge, this is the first study that analyzes garnet in such a way, and the results should prove valuable in the characterization of metamorphic rocks; in particular, to

distinguish the accessory crystalline mineral phases present in garnet.

Acknowledgments

We gratefully acknowledge the Vicerrectoría de Investigación y Extensión of the Universidad Industrial de Santander for the use of their research facilities (scanning electron microscopy and X-ray diffraction). We also thank the Microscopy and X-Rays laboratories at the Universidad Industrial de Santander - Guatiguará Technology Park, and their staff for the analytical service provided for data acquisition. The authors would also like to acknowledge the anonymous referees for their critical and insightful reading of the manuscript and are most grateful to the above-named people and institutions for support.

References

[1] Tissot, R.G., Microdiffraction applications utilizing a two-dimensional proportional detector. Powder Diffraction, 18(2), pp 86-90, 2003. DOI: 10.1154/1.1577354

[2] Flemming, R.L., Salzsauler, K.A., Sherriff, B. L. and Sidenko, N.V., Identification of scorodite in fine-grained, high-sulfide, arsenopyrite mine-waste using micro X-ray diffraction (μXRD). The Canadian Mineralogist, 43, pp. 1243-1254, 2005. DOI: 10.2113/gscanmin.43.4.1243

[3] Harwood, B.P., Flemming, R.L. and Stachel, T., Mapping a mantle xenolith using micro X-ray diffraction. Abstract #MA73B-09, American Geophysical Union, Spring Meeting, 2009.

[4] Catalano, J.G., Heald, S.M., Zachara, J.M. and Brown, Jr., G.E., X-ray microdiffraction study of Uranium speciation in contaminated vadose zone sediments from the Hanford Site, Washington. US Department of Energy Publications, [Online]. Paper 226, 2004. Available at http://digitalcommons.unl.edu/usdoepub/226

[5] Flemming, R.L., Micro X-ray diffraction (μXRD): A versatile technique for characterization of Earth and planetary materials. Canadian Journal of Earth Sciences, 44(9), pp. 1333-1346, 2007. DOI: 10.1139/E07-020

[6] Flemming, R.L., McCausland, P.J.A., Izawa, M.R. and Jacques, N., Reconnaissance micro-XRD studies of meteorites: Rapid in situ mineral identification and textural information. Abstract #2363, 38th Lunar and Planetary Science Conference, Houston, TX, 2007.

[7] Izawa, M.R.M., Flemming, R.L., Banerjee, N.R. and McCausland, P.J.A., Micro X-ray diffraction (μXRD) assessment of shock stage in enstatite chondrites. Meteoritics and Planetary Science, 46, pp 638-651, 2011. DOI: 10.1111/j.1945-5100.2011.01180.x

[8] Dähn, R., Popov, D., Schaub, Ph., Pattison, P., Grolimund, D., Mäder, U., Jenni, A. and Wieland, E., X-ray micro-diffraction studies of heterogeneous interfaces between cementitious materials and geological formations. Physics and Chemistry of the Earth, Parts A/B/C, 70-71, pp. 96-103, 2014. DOI: 10.1016/j.pce.2013.10.010

[9] Pereira, E., Ortíz, F. and Prichard, H., Contribución al conocimiento de las anfibolitas y dunitas de Medellín (Complejo Ofiolítico de Aburrá). DYNA, 73(149), pp. 17-30, 2006.

[10] Ríos, C.A., Castellanos, O.M., Ríos, V. y Gómez, C., Una contribución al estudio de la evolución tectono-metamórfica de las rocas de alta presión del Complejo Arquía, Cordillera Central, Andes Colombianos. Geología Colombiana, 33, pp. 3-22, 2008.

[11] Ruíz-Jiménez, E.C., Blanco-Quintero, I.F., Toro, L.M., Moreno-Sánchez, M., Vinasco, C.J., García-Casco, A., Morota, D. and Gómez-Cruz, A., Geochemistry and petrology of metabasites of the Arquía Complex (Santa Fe de Antoquia and Arquía River, Colombia): Geodynamic implications. Boletín de Ciencias de la Tierra, 32, pp. 65-80, 2012.

[12] Valencia-Morales, Y.T., Toro-Toro, L.M., Ruiz-Jiménez, E.C. and Moreno-Sánchez, M., Pressure-Temperature path of Arquía Group rocks (NW Colombia): A petrographic analysis from mineral assemblages. Earth Science Research Journal, 17(2), pp. 141-149, 2013. DOI: 10.1127/0077-7749/2013/0338

[13] Pardo-Trujillo, A. y Moreno-Sánchez, M., Estratigrafía del occidente colombiano y su relación con la evolución de la provincia ígnea Cretácea del Caribe Colombiano, VIII Congreso Colombiano de Geología, Manizales, Colombia, Agosto, 2001.

[14] Kerr, A., Marriner, G., Tarney, J., Nivia, A., Saunders, A., Thirlwall, M. and Sinton, C., Cretaceous basaltic terranes in Western Colombia: Elemental, chronological and Sr-Nd isotopic constraints on petrogenesis. Journal of Petrology, 38, pp. 677-702, 1997. DOI: 10.1093/petrology/38.6.677

[15] Kretz, R., Symbols for rock-forming minerals. American Mineralogist, 68, pp. 277-279, 1983. DOI: 10.2138/am.2010.3371

[16] Sawada, H., Electron density study of garnets: $Z_3Al_2Si_3O_{12}$ (Z = Mg, Fe, Mn, Ca) and $Ca_3Fe_2Si_3O_{12}$. Journal of Solid State Chemistry, 142(2), pp. 273-278, 1999. DOI: 10.1006/jssc.1998.7983

J.D. Bonilla-Jaimes, received his BSc. in Chemistry in 2010 from the Universidad Industrial de Santander, Bucaramanga, Colombia. He has been working in the X-Ray Laboratory at the Guatiguará Technological Park since 2012. He is member of the Research Group in Structural Chemistry at the School of Chemistry of the Universidad Industrial de Santander, Colombia and is a specialist in X-ray fluorescence and X-ray diffraction techniques and has extensive research experience in characterization of materials.
ORCID: 0000-0002-2079-8043

J.A. Henao-Martínez, received his BSc. in Chemistry in 1982 and MSc. in Chemistry in 1990 from the Universidad Industrial de Santander, Bucaramanga, Colombia. The Universidad de Los Andes, Mérida, Venezuela, awarded him a PhD. in Applied Chemistry in 1996. He has been working as a full-time Lecturer at the School of Geology in the Universidad Industrial de Santander, Colombia, since 1991 where he developed his university teaching over the past 23 years in the field of crystallochemistry. He undertook postdoctoral research at the Instituto Zuliano de Investigaciones (Venezuela) in 2006. He is currently the director of the Research Group in Structural Chemistry at the School of Chemistry of the Universidad Industrial de Santander and the director of the X-Ray Laboratory of the Guatiguará Technological Park. He is a specialist in material characterization in several X-ray diffraction techniques and has extensive research experience in the characterization of materials.
ORCID: 0000-0002-2887-1532

C. Mendoza-Luna, received her BSc. in Physics in 2012 from the Universidad Industrial de Santander, Bucaramanga, Colombia. She is currently undertaking a MSc. in Physics. She has been working in the Microscopy Laboratory at the Guatiguará Technological Park since 2012. She is member of the Research Group in Optics and Signal Processing at the School of Physics at the Universidad Industrial de Santander, and is a specialist in scanning electron microscopy and atomic force microscopy techniques. Her research areas of interest include nanometrology, nanolithography and optoelectronics.
ORCID: 0000-0002-7461-3585

O.M. Castellanos-Alarcón, received his BSc. in Geology in 1999 from the Universidad Industrial de Santander, Bucaramanga, Colombia. He was awarded an MSc. in Geology from the Shimane University, Matsue, Japan, in 2001. He has been working as a full-time Lecturer on the Geology Program (Universidad de Pamplona) since 2003, where he has developed his professional university teaching over the past 11 years in the field of Mineralogy, Metamorphic Petrology and fieldwork on crystalline basement complexes in different areas of Colombia. He is

member of the Research Group on Basic and Applied Geology at the School of Geology, Universidad Industrial de Santander. He is specialist in mineralogy, experimental geology, petrology and the geochemistry of metamorphic rocks, and has extensive research experience in geological mapping, experimental and environmental mineralogy and metamorphic petrology.
ORCID: 0000-0003-0620-0540

C.A. Ríos-Reyes, received his BSc. in Geology in 1989 and his Post-graduate Diploma in University Teaching in 1995 from the Universidad Industrial de Santander, Bucaramanga, Colombia. He was awarded an MSc. in Geology from the Shimane University, Matsue, Japan, in 1999. He was awarded a PhD. in Applied Sciences from the University of Wolverhampton, Wolverhampton, England, in 2008. He has been working as a full-time Lecturer of the School of Geology (Universidad Industrial de Santander) since 1992, and has been teaching in the fields of Mineralogy, Metamorphic Petrology and fieldwork on crystalline basement complexes in different areas of Colombia for the past 22 years. He is currently the director of the Research Group in Basic and Applied Geology at the School of Geology of the Universidad Industrial de Santander and the director of the Microscopy Laboratory of the Guatiguará Technological Park. He is specialist in mineralogy, experimental geology, petrology and geochemistry of metamorphic rocks and has extensive research experience in geological mapping, experimental and environmental mineralogy and metamorphic petrology.
ORCID: 0000-0002-3508-0771